geoconvention
Calgary • Canada • May 13-17 2019

Permeability estimation from hydraulic fracturing induced microseismicity: Effect of fracture growth

Himanshu Barthwal and Mirko van der Baan
University of Alberta

Summary

Hydraulic fracturing of low-permeability hydrocarbon reservoirs triggers microseismic events which are often used to estimate the fracture dimensions. The microseismic event clouds have also been used to estimate the permeability of fractured rocks by attributing the triggering front of microseismicity observed in the distance versus time plots to the pore pressure diffusion process. Assuming a penny-shaped hydraulic fracture and using a material balance equation with a propagation criterion, we show that the rate of fracture growth can be much faster than that of the pore pressure diffusion in low-permeability hydrocarbon reservoirs like shales and tight sands. Therefore, the observed triggering front may be explained by the crack tip propagation. Thus, the diffusivity estimates obtained by fitting a pore pressure diffusion front to the triggering front can lead to overestimation by many orders of magnitude.

Introduction

Hydraulic fracturing is often performed to enhance the permeability of hydrocarbon bearing tight sands and shales. This process is accompanied by microseismic events which are triggered by creation/reactivation of a fracture network. Monitoring of these microseismic events is used to map fracture orientation and dimensions (Maxwell et al., 2002; Rutledge and Phillips, 2003; Cipolla et al., 2011). Shapiro et al., 2006 and Shapiro and Dinske, 2009 suggest estimating the formation permeability using the microseismic data. Their permeability estimates depend upon an apparent diffusivity parameter which is obtained from the triggering front of microseismicity observed in the distance versus time plots. Grechka et al., 2010 use the method of Shapiro et al., 2006 to compute the permeability of hydraulically fractured tight sands. This method assumes that fluid loss into the formation is the dominant phenomenon triggering microseismicity. However, it neglects the role of fracture propagation in shaping the microseismic cloud.

Barthwal and Van der Baan (2017) model the elastic stress changes and the pore pressure diffusion profiles due to a stationary hydraulic fracture cavity. They conclude that the elastic stress changes near the tip of the fracture cavity facilitate shear slip failure thereby triggering microseismic events. In this study, we show that during the injection period in low-permeability hydrocarbon bearing formations, the observed triggering front may be attributed to fracture propagation rather than pore pressure diffusion. Moreover, neglecting the fracture growth leads to overestimation of hydraulic diffusivity.

Method

We assume a vertical penny-shaped hydraulic fracture cavity with equal height and length and an aperture which is much smaller than the other two major axes. The same model was used by Barthwal and Van der Baan, 2017. In order to compute fracture length growth over time, we apply a material balance equation together with a fracture propagation criterion. According to the material balance equation, we get (Harrington and Hannah, 1975; Economides and Nolte, 2003)

$$Q_i t = \frac{4}{3}\pi abc + \pi b h_f C_l \sqrt{2t}\,, \tag{1}$$

where Q_i is the average injection rate of treatment fluid, h_f is the fracture height, a, b, and c are the semi-axes of our penny-shaped model, t is the injection time, and C_l is the fluid leak-off coefficient. For the penny-shaped model, $b = c = L$ where L is the half-length of the hydraulic fracture. Therefore, the fracture height is $h_f = 2L$. The maximum fracture aperture is $2a$.

Assuming that the fracture propagates under constant stress intensity factor, the maximum aperture is given as (Olson, 2003)

$$2a = K_{ic}\frac{(1-\nu^2)}{E\sqrt{\pi/8}}\sqrt{2L}\,, \tag{2}$$

where K_{ic} is the fracture toughness, E is the Young's modulus, and ν is the Poisson's ratio. Substituting aperture a from equation 2 in equation 1, and using $b = c = L$ and $h_f = 2L$ we get

$$\left[\frac{8\sqrt{\pi}K_{ic}}{3E'}\right]^2 L^5 - \left[2\pi C_l\sqrt{2t}\,\right]^2 L^4 + \left[4\sqrt{2}\pi C_l Q_i t^{3/2}\,\right]L^2 - [Q_i t]^2 = 0\,, \tag{3}$$

where

$$E' = \frac{E}{1-\nu^2}\,. \tag{4}$$

The smallest positive real root of equation 3 gives the half-length of the fracture as a function of time.

The distance L of the pore pressure diffusion front from a point injector is computed as (Shapiro et al., 2002; Rothert and Shapiro, 2003)

$$L = \sqrt{4\pi ct}\,, \tag{5}$$

where c is the hydraulic diffusivity given as (Rice and Cleary, 1976; Segall, 1985)

$$c = \frac{k}{\eta\Phi\beta}\,, \tag{6}$$

where k is the permeability, Φ is the porosity and β is the fluid compressibility.

Table 1: Parameters used for modeling rate of fracture length growth, and the triggering front due to fluid diffusion from a point injector

Parameter	Value and unit
Fracture toughness, K_{ic}	10 MPa$\sqrt{m}$
Young's modulus, E	40 GPa
Poisson ratio, ν	0.23
Leak-off coefficient, C_l	0.00003 m/s$^{1/2}$
Volume injection rate, Q_i	0.15 m^3/s
Porosity, Φ	0.1
Permeability, k	100 nanodarcy or 9.9*10^{-20} m^2
Compressibility gas, β_g	10^{-5} Pa^{-1}
Compressibility water, β_w	3*10^{-10} Pa^{-1}
Viscosity gas, η_g	2*10^{-5} Pas
Viscosity water, η_w	10^{-3} Pas
Diffusivity gas, C_g	5*10^{-9} m^2/s
Diffusivity water, C_w	3.3*10^{-6} m^2/s

Results

We compare the rate of fracture length growth and the pore pressure diffusion fronts to understand their role in shaping the triggering front observed in the distance versus time plots of microseismic events. The fracture length is computed using equation 3 whereas the distance of the pore pressure diffusion front from a point injector is computed using equation 5 where c is the hydraulic diffusivity. We list the typical values of compressibility and viscosity for water and gas, porosity and the permeability for shale samples (Vermylen, 2011), and the corresponding diffusivity computed using equation 6 in Table 1. Since diffusivity depends upon the permeability and porosity of the rock as well as the viscosity and compressibility of the formation fluid, the diffusivity of water is three orders of magnitude higher than that of gas. Figure 1 shows the pore pressure diffusion fronts and the crack tip length as a function of time. The pore pressure diffusion fronts in the case of water and gas for typical values of lab-measured diffusivity (dashed red and solid green lines) lag the crack tip propagation (solid blue line). Even when the lab-measured diffusivity values are increased by 10^4 times for water ($3.3*10^{-2}$ m^2/s) and 10^6 times for gas ($5*10^{-3}$ m^2/s), the crack tip propagation (blue curve) is much faster than the pore pressure diffusion fronts (dashed magenta and solid black lines).

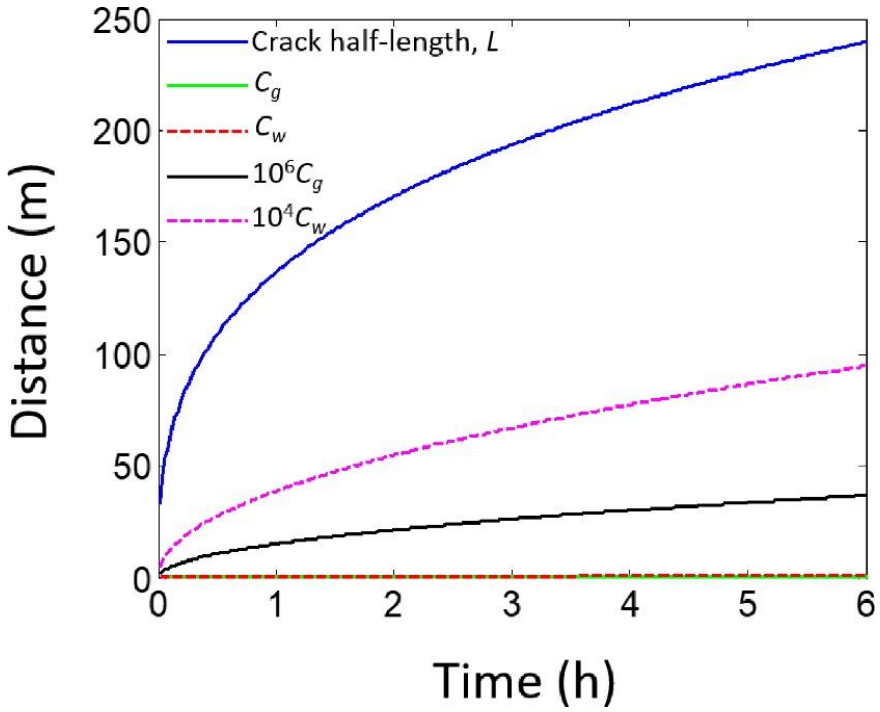

Figure 1: Distance of hydraulic fracture tip and pore pressure diffusion front from a point injector as a function of time. Solid blue line shows fracture half-length. Dashed red and magenta lines show distance of diffusion front in case of water for in-situ (c_w in Table 1) and scaled up (10^4 times c_w) diffusivity respectively. Solid green and black lines show distance of diffusion front in case of gas for in-situ (c_g in Table 1) and scaled up (10^6 times c_g) diffusivity respectively.

Discussions

The evolution of the fracture tip over time as given by equation 3 depends upon the average injection rate of treatment fluid (Q_i), the fluid leak-off coefficient (C_l), the fracture toughness (K_{ic}), and the elastic constants of the medium (plane strain modulus, E' given in equation 4). We test the sensitivity of the fracture length growth over time with respect to each of these four parameters by varying them individually while keeping all others constant. We find that the rate of fracture length growth is much faster than that of the pore pressure diffusion

front for typical values of these parameters in the case of hydraulic fracturing of low-permeability hydrocarbon reservoirs. Thus, at any time during fracture growth, the microseismic events near the crack tip triggered by elastic stress changes would be farthest from the injection point. In other words, the crack tip propagation can be used as a proxy for the triggering front of microseismicity observed in the distance versus time plots.

Shapiro et al. (1997), Shapiro et al. (2002), and Rothert and Shapiro (2003) argue that the triggering front of microseismicity can be used to estimate the hydraulic diffusivity of rocks leading to the seismicity based reservoir characterization (SBRC) approach. The main assumption of SBRC is that the fluid induced microseismicity is triggered in critically stressed rocks solely due to pore pressure diffusion (Shapiro et al., 2002, 2005). Such an interpretation is more apt to highly permeable rocks or rocks with open fractures where pore pressure diffusion is the dominant mechanism inducing seismicity, e.g., saltwater injection into highly permeable aquifers (Hornbach et al., 2015; Keranen et al., 2014) since injection occurs below the fracture gradient of the rock. In this case, the fracture volume, as described by the first term on the right-hand side of material balance equation (equation 1), will be negligibly small compared to the contribution of the fluid leak-off terms, resulting in most injected fluids flowing into the surrounding rocks.

In the case of hydraulic fracturing of low-permeability rocks, the growth rate of fracture length is much faster than that of the pore pressure diffusion front. As shown in Figure 1, we need to scale up the hydraulic diffusivity by multiple orders of magnitude to match the fracture length growth over time. Therefore, the diffusivity estimated by fitting the triggering front by pore pressure diffusion fronts will lead to overestimation.

Conclusions

The spatiotemporal distribution of microseismicity observed during hydraulic fracturing is shaped not only by pore pressure diffusion but also by the opening of the fracture cavities which can trigger events due to elastic stress perturbations. In this study, we show that in low-permeability hydrocarbon reservoirs like shales and tight sands, crack tip propagates much faster than the pore pressure diffusion fronts and can be used as a proxy for the triggering front of microseismicity. Consequently, the apparent diffusivity computed by fitting a pore pressure diffusion front to the observed triggering front is overestimated by several orders of magnitude.

Acknowledgments

We thank the sponsors of the Microseismic Industry Consortium for project funding.

References

Barthwal, H., and M. van der Baan, 2017, Stress perturbations and microseismicity induced by hydraulic fracturing: 51st US Rock mechanics/Geomechanics Symposium, American Rock Mechanics Association. Paper 17-136. San Francisco.

Cipolla, C., S. Maxwell, M. Mack, and R. Downie, 2011, A practical guide to interpreting microseismic measurements: SPE 144067.

Economides, M. J., and K. G. Nolte (Eds.), 2003, Reservoir Stimulation, 3rd ed.: John Wiley, Hoboken, N. J., 5-1-5-14.

Grechka, V., P. Mazumdar, and S. A. Shapiro, 2010, Predicting permeability and gas production of hydraulically fractured tight sands from microseismic data: Geophysics, 75(1), B1-B10.

Harrington, L., and R. R. Hannah, 1975, Fracturing Design Using Perfect Support Fluids for Selected Fracture Proppant Concentrations in Vertical Fractures: SPE 5642, presented at the SPE Annual Meeting, Dallas, Texas, USA.

Hornbach, M. J., H.R. DeShon, W. L. Ellsworth, B. W. Stump, C. Hayward, C. Frohlich, H. R. Oldham, J. E. Olson, M. B. Magnani, C. Brokaw, and J. H. Luetgert, 2015, Causal factors for seismicity near Azle, Texas. Nature Communications, 6, 6728.

Keranen, K., M. Weingarten, G. Abers, B. Bekins, and S. Ge, 2014, Sharp increase in central Oklahoma seismicity since 2008 induced by massive wastewater injection: Science, 345(6195), 448-451.

Maxwell, S. C., T. I. Urbancic, N. Steinsberger, and R. Zinno, 2002, Microseismic Imaging of Hydraulic Fracture Complexity in the Barnett Shale, SPE-77440, SPE Annual Technical Conference and Exhibition, San Antonio, Texas.

Olson, J. E., 2003, Sublinear scaling of fracture aperture versus length: an exception or the rule? Journal of Geophysical Research Solid Earth,108(B9).

Rice, J.R., and M. P. Cleary, 1976, Some basic stress diffusion solutions for fluid saturated elastic porous media with compressible constituents: Reviews of Geophysics and Space Physics, 14, 227-241.

Rothert, E., and S. Shapiro, 2003, Microseismic monitoring of borehole fluid injections: Data modeling and inversion for hydraulic properties of rocks: Geophysics, 68(2), 685-689.

Rutledge, J. T., and W. S. Phillips, 2003, Hydraulic stimulation of natural fractures as revealed by induced microearthquakes: Geophysics, 68(2), 441-452.

Segall, P., 1985, Stress and subsidence resulting from subsurface fluid withdrawal in the epicentral region of the 1983 Coalinga earthquake: Journal of Geophysical Research, 90, 6801-6816.

Shapiro, S.A., E. Huenges, and G., Borm, 1997, Estimating the crust permeability from fluid-injection-induced seismic emission at the KTB site: Geophysical Journal International, 131, F15-F18.

Shapiro, S. A., E. Rothert, V. Rath, and J. Rindschwentner, 2002, Characterization of fluid transport properties of reservoirs using induced microseismicity: Geophysics, 67, 212-220.

Shapiro, S., S. Rentsch, and E. Rothert, 2005, Characterization of hydraulic properties of rocks using probability of fluid-induced microearthquakes, Geophysics, 70, F27-F33.

Shapiro, S. A., C. Dinske, and E. Rothert, 2006, Hydraulic-fracturing controlled dynamics of microseismic clouds: Geophysical Research Letters, 33, L14312.

Shapiro, S. A., and C. Dinske, 2009, Scaling of seismicity induced by nonlinear fluid rock interaction: Journal of Geophysical Research, 114, B09307.